ARCHIVES OF ELECTRICAL ENGINEERING VOL. 59(1-2), 87-98 (2010)

DOI 10.2478/s10171-010-0007-y

# Synthesis and CAD of permanent magnet DC brushless motors

MIROSŁAW DĄBROWSKI[1], ANDRZEJ RUDEŃSKI[2]

[1]*Instytut Elektrotechniki i Elektroniki Przemysłowej, Politechnika Poznańska*
*Piotrowo 3A, 60-965 Poznań, Poland*
*e-mail: miroslaw.dabrowski@put.poznan.pl*

[2]*Zakład Maszyn Elektrycznych, Instytut Elektrotechniki*
*Pożaryskiego 28, 04-703 Warszawa, Poland*
*e-mail: a.rudenski@iel.waw.pl*

(Received: 25.05.2010, revised: 09.06.2010)

**Abstract:** The paper presents an algorithm and software for the optimal design of permanent magnet brushless DC motors. Such motors are powered by DC voltage sources via semiconductor switches connected to the motor phase belts. The software is adjusted to the design of motors with NdFeB high energy density magnets. An attention has been given to issues important in the design of the motors, i.e., permanent magnet selection, structure of magnetic circuit, and armature windings. Particularly, precision of calculation of the permanent magnet operating point, visualization of selection process of the winding belts, and magnetic circuit dimensioning have been investigated. The authors have been trying to make the equations more specific and accurate than those presented in the literature. The user software interface allows changes in the magnetic circuit dimensions, and in the winding parameters. It is possible to examine simultaneously the influence of these changes on the calculation results. The software operates both with standard and inverted (outer rotor) motor structure. To perform optimization, a non-deterministic method based on the evolution strategy $(\mu + \lambda)$ – ES has been used.

**Key words:** brushless DC motor, design of electric machines, optimization

## 1. Introduction

DC motors with electronic commutation (powered with semiconductor switches) are in English-language literature referred to as the *permanent magnet DC brushless motors*. They belong to the group of motors with the rotational speed regulated by the switching frequency of currents in the armature winding belts.

Fast development of brushless motors with electronic commutation can be observed after the invention of samarium-cobalt permanent magnets (Sm-Co) in the 70s of the last century and after mastering in the 80s the production of NdFeB magnets with high magnetic energy density. Main difficulty in their design arises from the lack of a full analytical theory describing all relevant phenomena occurring in them [8-12].

Two control strat egies are used in electromechanical drives with brushless DC motors powered from the constant voltage source via a semiconductor switching system: a trapezoidal or rectangular waveform control and a sinusoidal waveform control. All these terms refer to approximate shapes of currents in the motor winding belts. The presented algorithm of computation and associated computer program are designed for motors powered with rectangular waveforms.

An attention has been given to some specific issues important in the design of the discussed motors, i.e., permanent magnet selection, structure of magnetic circuit, and armature windings. Particularly, high precision of calculation of the permanent magnet operating point, visualization of selection process of the winding belts, and magnetic circuit dimensioning have been investigated. The elaborated computer program can be used in the design of motors both with the classical structure, i.e., magnets placed on the external rotor surface and the inverted structure, i.e., internal stationary armature and magnets placed on the inner surface of the external rotor. A non-deterministic optimization procedure for the motor synthesis has been employed.

## 2. Design calculation algorithm

The main difficulty in the design of brushless DC motors is an incomplete theory describing complex phenomena occurring in these motors, i.e., complex shapes of currents, induced voltages, and electromagnetic torque. Calculation of the winding power losses and consequently the magnetic core and permanent magnet sizing is also a complex task. However, the authors have been trying to make the equations more specific and accurate than those presented in the literature. The computer program created on the basis of the elaborated algorithm serves as a fast and effective design tool of DC brushless motors. It consists of the following calculations:

- preliminary calculations (electromagnetic torque and current in the motor windings excited by rectangular waveforms);
- calculations of the main dimensions of the magnetic circuit;
- iterative procedure for calculations of the magnetic circuit and location of the permanent magnet operating point at no-load;
- selection of the winding configuration and the number of armature slots per pole;
- calculation of the number of turns per phase of the armature winding and selection of wire dimensions;
- iterative procedure for calculations of the magnetic circuit with consideration of its nonlinearity and location of the permanent magnet operating point at rated load;
- calculations of the winding resistance, components of power losses, and motor efficiency;
- calculations of the over-current ratio, i.e. maximum permissible current-to-rated current ratio, in order to prevent permanent magnets to be demagnetized.

In the magnetic circuit and the permanent magnet operating point calculations only two components of the permanent magnet leakage permeance (flux) have been considered, i.e., magnet side-to-rotor core and magnet front surface-to-rotor core [3-6].

Proper selection of the winding structure with respect to the numbers of slots per pole is very important in engineering practice. Permissible numbers of slots and poles, which assure reduction of the torque ripple (cogging torque) and torsional vibrations, are listed in Tab. 1.1)

In Figure 1 a block diagram (flow chart) of the created computer program is presented. A block realizing the iterative loop, which is crucial for the calculation of the efficiency, has been indicated.

Table 1. Recommended numbers of armature slots $\dot{Z}_t$ and poles $p$ that assure minimization of the torque ripple (cogging torque)

| Number of slots to number of poles ratio | | | | | | | | | | | | | | | |
|---|---|---|---|---|---|---|---|---|---|---|---|---|---|---|---|
| 0.75 | | 1.125 | | 1.5 | | 2.25 | | 3 | | 3.75 | | 4.5 | | 5.25 | |
| $\dot{Z}_t$ | $p$ | $\dot{Z}_t$ | $p$ | $\dot{Z}_t$ | $p$ | $\dot{Z}_t$ | $p$ | $\dot{Z}_t$ | $p$ | $\dot{Z}_t$ | $p$ | $\dot{Z}_t$ | $p$ | $\dot{Z}_t$ | $p$ |
| 3 | 4 | 9 | 8 | 3 | 2 | 9 | 4 | 6 | 2 | 15 | 4 | 9 | 2 | 21 | 4 |
| 6 | 8 | 18 | 16 | 6 | 4 | 18 | 8 | 12 | 4 | 30 | 8 | 18 | 4 | 42 | 8 |
| 9 | 12 | 36 | 32 | 9 | 6 | 27 | 12 | 18 | 6 | 45 | 12 | 27 | 6 | | |
| 12 | 16 | | | 12 | 8 | | | 24 | 8 | | | 36 | 8 | | |
| 15 | 20 | | | 15 | 10 | | | 30 | 10 | | | | | | |
| 18 | 24 | | | 18 | 12 | | | | | | | | | | |
| 21 | 28 | | | 21 | 14 | | | | | | | | | | |
| 24 | 32 | | | 24 | 16 | | | | | | | | | | |

## 3. Determination of permanent magnet operating point

In brushless DC motors the determination of the permanent magnet operating point is more complex than in DC brush motors or in line start synchronous motors (without speed control). This point must be determined not only for rated power, but also at no-load state and at overload.

The operating points have been determined analytically for the selected conditions – especially for the over-current at starting. A shape of the demagnetization characteristics, magnets-leakage flux and armature reaction have been taken into considerations.

---

1) The cogging torque is reduced if the *least common multiple* (LCM) of the stator slots and rotor poles is high, i.e., LCM($Z_t$, $2p$) takes maximum value. For example, the motor with 36 slots and 2 poles (LCM = 36) has higher amplitude of the cogging torque than the motor with 36 slots and 10 poles (LCM = 180). On the other hand, the acoustic noise of magnetic origin produced by the second motor is higher [13].

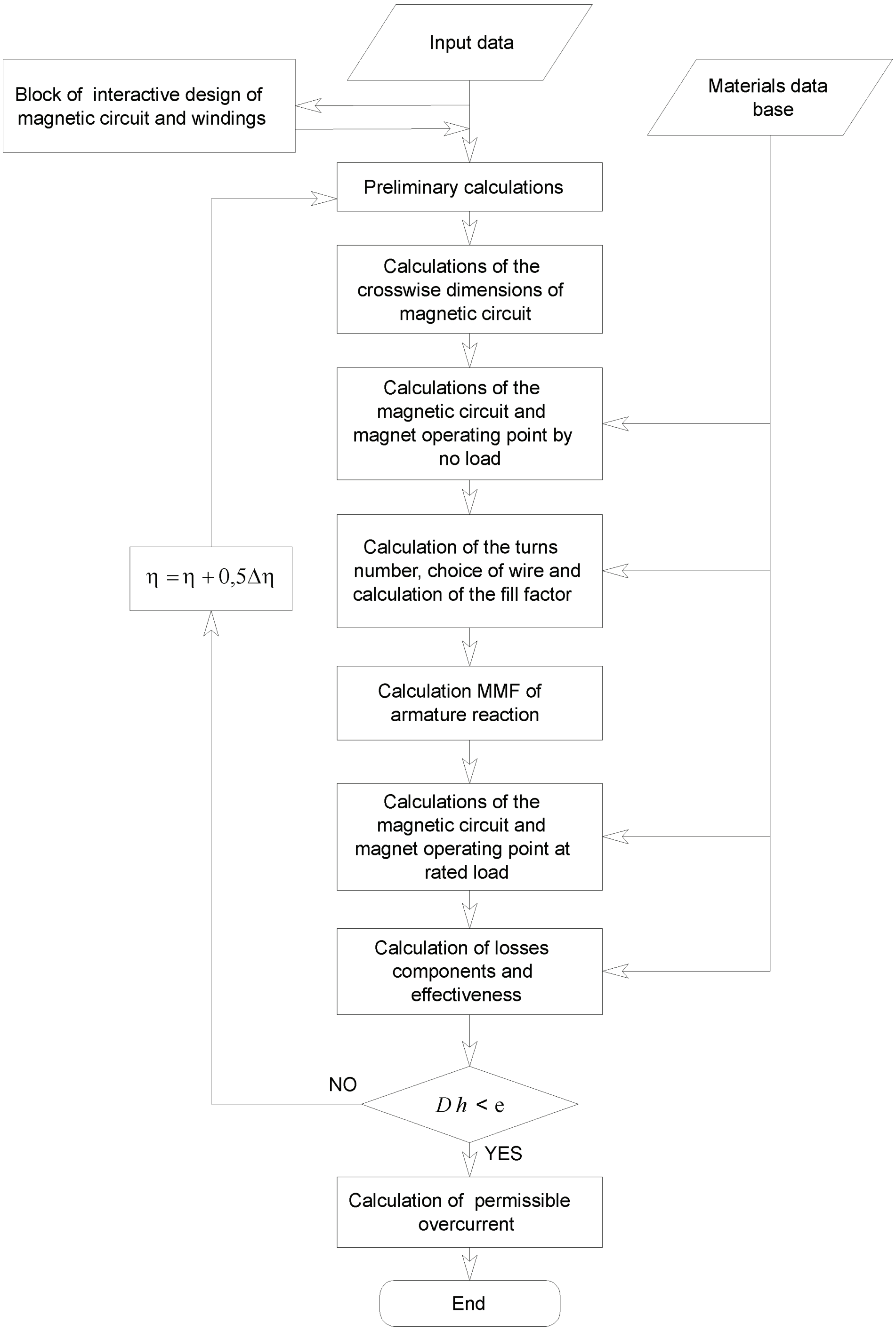

Fig. 1. Flow chart of the motor calculation

The magnet operating points determined at no-load and at rated load have been presented in Fig. 2. At no-load, more accurately, at zero-current state, the coordinates of the magnet operating point have been calculated using the following equations:

$$\Theta_A = \Theta_{id}\left(1 - \frac{1}{1 - u_i \dfrac{\Phi_r}{\Theta_{id}}}\right), \tag{1}$$

$$\Phi_A = \Phi_r \frac{\Theta_{id}}{\Theta_{id} - u_i \Phi_r}, \tag{2}$$

$$u_i = 2\ k_C\, \delta \frac{k_{ns}}{\mu_0\, \alpha_i\, \tau\, L}, \tag{3}$$

where: $k_{ns}$ is the saturation coefficient of the magnetic circuit; $k_c$ is the Carter's coefficient; $\delta$ is the air gap thickness; $\tau$ is the pole pitch; $\alpha_i$ is the magnet arc-to pole pitch ratio; $L$ is the core axial length; $u_i$ is a coefficient of inclination of the motor magnetic circuit characteristic. Remaining symbols are given in Fig. 2.

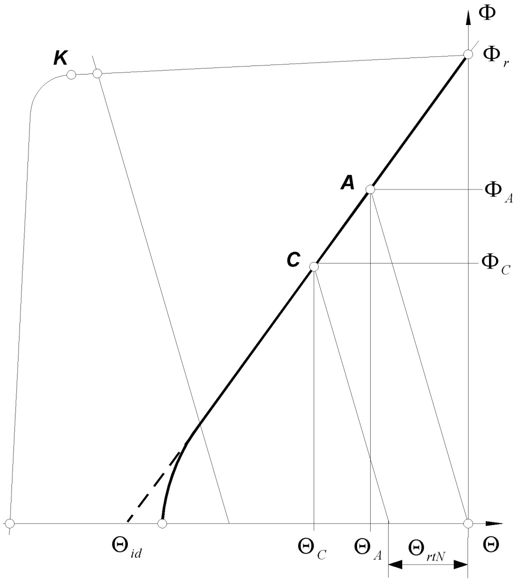

Fig. 2. Permanent magnet operating points: *A* – at no load; *C* – at rated power

The coordinates of the magnet operating point determined for the rated load have been calculated according to the following formulae:

$$\Phi_C = \Phi_r \left( \frac{1 - \dfrac{\Theta_{rtN}}{\Theta_{id}}}{1 - u_i \dfrac{\Phi_r}{\Theta_{id}}} \right), \tag{4}$$

$$\Theta_C = -u_i \Phi_C - \Theta_{rtN} , \tag{5}$$

where $\Theta_{rtN}$ is the MMF of the armature reaction.

In Fig. 2 the knee point of the demagnetization curve has been marked with the letter *K*. The coordinates of this point are then introduced to the material data base and are used for calculation of the over-current coefficient of the motor.

The main drawback of sintered magnets NdFeB is a strong sensitivity of remanence (residual flux density) and coercivity on the temperature of the magnet. Therefore, their values must be corrected in further calculations by temperature coefficients $k_{TBr}$, $k_{THci}$ for remanence and coercivity, i.e.,

$$B_r^t = B_r^{20} \left[ 1 + k_{TBr} \left( \frac{t - 20}{100} \right) \right], \tag{6}$$

$$H_{id}^t = H_{id}^{20} \left[ 1 + k_{THci} \left( \frac{t - 20}{100} \right) \right], \tag{7}$$

where: $B_r^{20}$ and $H_{id}^{20}$ are remanence and coercivity at room temperature of 20°C, respectively; $k_{TBr}$, $k_{THci}$ are temperature coefficients of remanence and coercivity expressed in [%/°C]; and $t$ is the magnet operating temperature.

Corrected remanence and coercivity values appear in formulae (1)-(5), while MMFs in these formulae are calculated on the basis of the corrected coercivity value.

A flow chart for the iterative procedure of the magnetic circuit analysis and calculation of the coordinates of the magnet operating point is presented in Fig. 3.

## 4. Interactive selection of magnetic circuit dimensions and windings parameters

The objective of the authors was to create a user friendly computer program. Correction of magnetic circuit dimensions, winding structure and other parameters is therefore possible during the whole design process. The software user-interface allows for introducing changes of these values in interactive way and immediate visualization of their influence on the motor parameters [1].

It is possible to introduce changes to all transverse dimensions of the stator and rotor core including the number of slots and their dimensions, dimensions of slot openings, number of slots per pole per phase, coil span, magnet angle and its thickness.

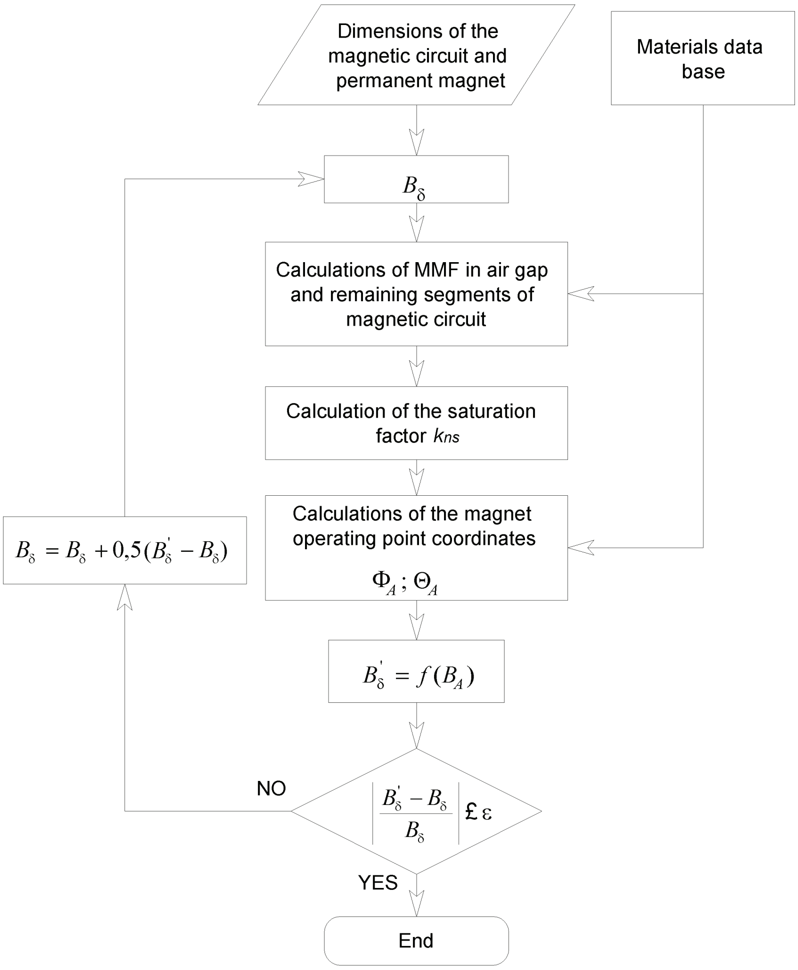

Fig. 3. Flow chart for the iterative procedure of the magnetic circuit analysis and calculation of coordinates of the magnet operating point

The elaborated program allows for applying any winding structures – also those with fractional numbers of slots per pole per phase. It should be emphasized that windings with fractional number of slots per pole per phase are nowadays frequently used, especially in motors with the inverted geometry (i.e., those with inner stationary armature and external ring-shaped rotor with magnets placed on its inner surface). Moreover, windings with fractional number of slots per pole per phase are favorable to obtain small torque ripples.

After introducing relevant changes to motor dimensions in the window for interactive design of the magnetic circuit and winding structure, an image of the motor cross-section with winding diagram is drawn in this window on the computer screen including real geometric proportions. Two examples of this window are shown in Figs. 4 and 5, for the classic and for inverted motor structures, respectively.

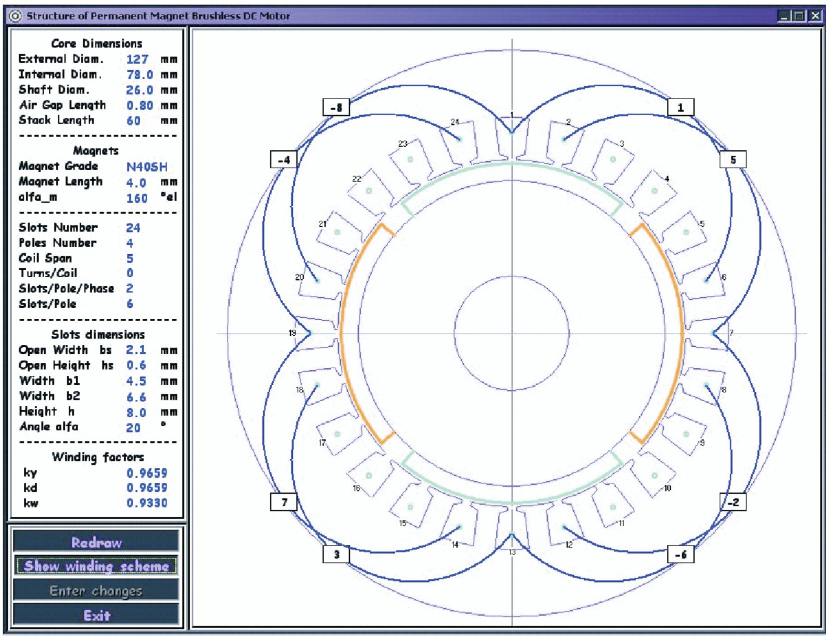

Structure of Permanent Magnet Brushless DC Motor

```
        Core Dimensions
External Diam.     127   mm
Internal Diam.     78.0  mm
Shaft Diam.        26.0  mm
Air Gap Length     0.80  mm
Stack Length       60    mm
-----------------------------
           Magnets
Magnet Grade       N40SH
Magnet Length      4.0   mm
alfa_m             160   °el
-----------------------------
Slots Number       24
Poles Number       4
Coil Span          5
Turns/Coil         0
Slots/Pole/Phase   2
Slots/Pole         6
-----------------------------
        Slots dimensions
Open Width   bs    2.1   mm
Open Height  hs    0.6   mm
Width  b1          4.5   mm
Width  b2          6.6   mm
Height  h          8.0   mm
Angle alfa         20    °
-----------------------------
        Winding factors
 ky                0.9659
 kd                0.9659
 kw                0.9330
```

Fig. 4. Window for interactive design of magnetic circuit and windings of the motor with internal rotor

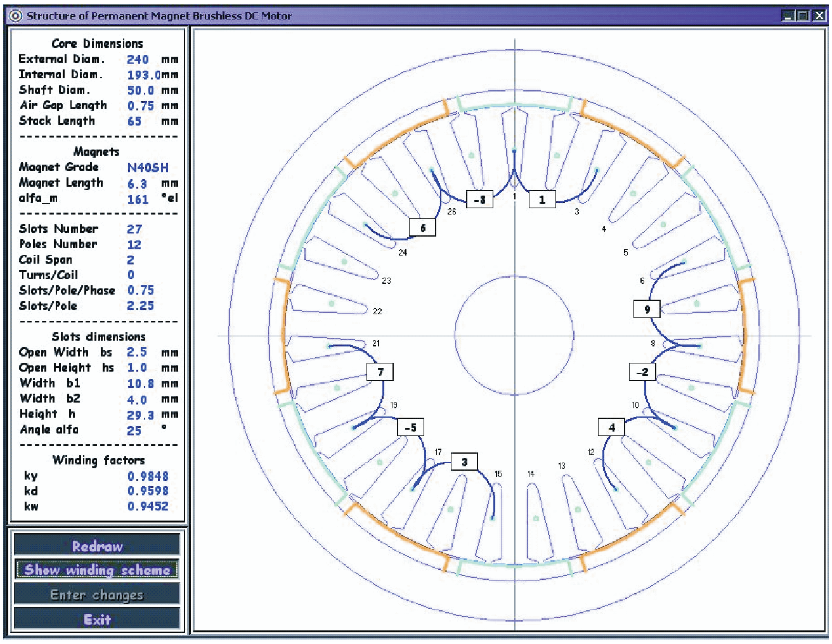

Structure of Permanent Magnet Brushless DC Motor

```
        Core Dimensions
External Diam.     240   mm
Internal Diam.     193.0mm
Shaft Diam.        50.0  mm
Air Gap Length     0.75  mm
Stack Length       65    mm
-----------------------------
           Magnets
Magnet Grade       N40SH
Magnet Length      6.3   mm
alfa_m             161   °el
-----------------------------
Slots Number       27
Poles Number       12
Coil Span          2
Turns/Coil         0
Slots/Pole/Phase   0.75
Slots/Pole         2.25
-----------------------------
        Slots dimensions
Open Width   bs    2.5   mm
Open Height  hs    1.0   mm
Width  b1          10.8  mm
Width  b2          4.0   mm
Height  h          29.3  mm
Angle alfa         25    °
-----------------------------
        Winding factors
 ky                0.9848
 kd                0.9598
 kw                0.9452
```

Fig. 5. Window for interactive design of magnetic circuit and windings of the motor with external rotor

Furthermore, the program offers visual presentation of phase and line EMF's, and the shaft torque as functions of the rotor position angle (Fig. 6). This visualization is helpful from many aspects. Among them are: correct assessment of the magnet angle $\beta$, windings structure and their parameters, number of slots per pole per phase, and the coil span. These parameters have essential influence on the torque pulsation. Approximate voltage and torque waveforms shown in Fig. 6 have been calculated using the, so called, "*Blv*" method, presented among others in [12].

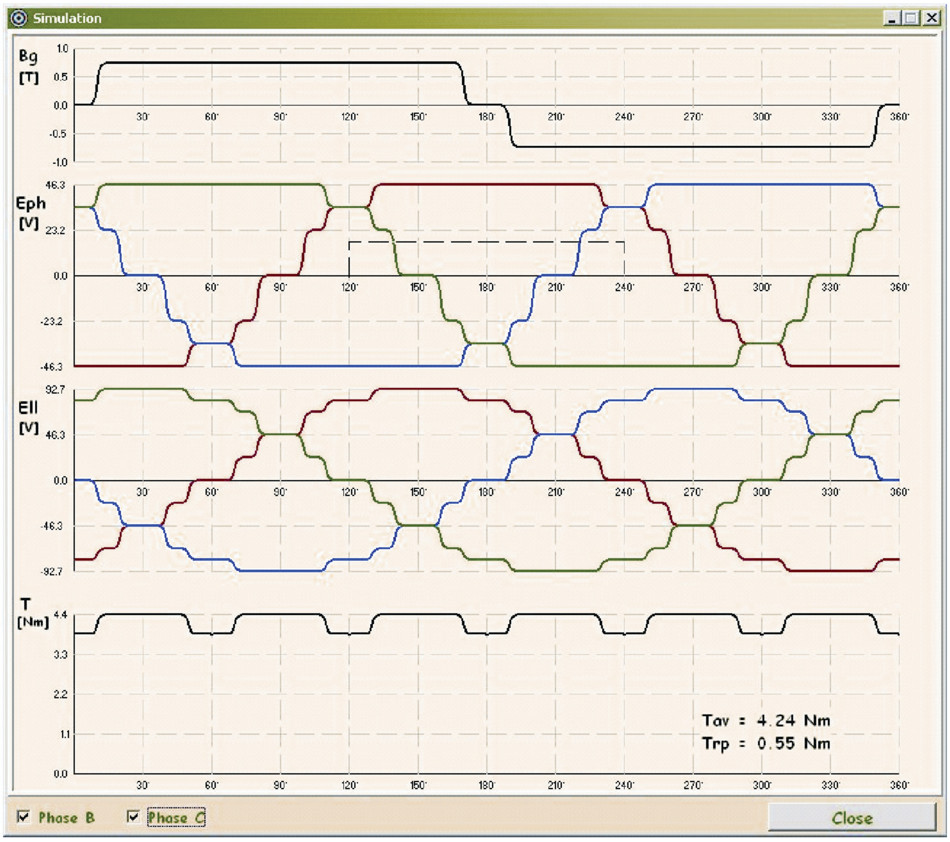

Tav = 4.24 Nm
Trp = 0.55 Nm

☑ Phase B ☑ Phase C

Fig. 6. Program window with simulation results of the induced voltages and torque waveforms

## 5. Optimization procedure

After preliminary synthesis the motor has been optimized. A non-deterministic procedure based on the evolution strategy ($\mu + \lambda$) – ES has been used [7, 15]. Minimization of costs of active materials necessary to produce the motor has been chosen as the optimization criterion (objective function). Selecting this criterion the following circumstances have been taken into account:

- manufacturing costs of brushless DC motors that mainly arise from the costs of high energy density permanent magnets and from the costs of electrical steel with low specific losses at high frequency, which is necessary to use in high-speed motors;
- costs of energy losses during exploitation of this type of motors – they have in fact a minor effect in the case of small brushless motors.

Brushless DC motors with electronic commutation are the highest efficiency motors of conventional construction. Usually they are used in variable frequency drives.

An algorithm for calculation of the selected objective function includes seven independent variables: the stator core diameter $D$ inner or outer diameter depending on the type of the motor geometry; the armature core length $L$; the external core diameter $D_e$ (armature or rotor diameter depending on the motor geometry); the armature slot width $b_Q$; the armature tooth height $h_t$; the magnet angle $\beta$; and the magnet thickness $b_m$.

Constraints are imposed on the following construction and exploitation parameters: the minimal efficiency $\eta_{\min}$; the maximal current density in the armature winding $j_{\max}$; the maximal fill factor of the armature slot $k_{z\max}$; the maximum value of the flux density in tooth and yokes $B_{\max}$; the minimal over-current coefficient $k_{\min}$.

In the optimization procedure a population of $\mu$ initial solutions is formed by a set of solution vectors with components, which are generated as independent random variables with the prescribed variation range according to the formula:

$$x_j = x_{j,lo} + R \cdot \left(x_{j,up} - x_{j,lo}\right) \quad j = 1, 2, \ldots, n, \tag{8}$$

where: $x_{j,lo}$ and $x_{j,up}$ is the lower and the upper variation limit, respectively, of the $j$-th independent variable; $R$ is the random variable with the uniform distribution in range [0, 1]; $n$ is the number of independent variables.

Evaluation of solutions in the initial population and solutions created by the optimization procedure is performed with the aid of the fitness function, i.e. the objective function supplemented by the penalty component due to violation of constraints [15]. The fitness function $f(\mathbf{x})$ has the following form:

$$f(\mathbf{x}) = f_c(\mathbf{x}) + \sum_{i=1}^{m} w_i \cdot g_i(\mathbf{x}); \quad g_i(\mathbf{x}) \geq 0\,, \tag{9}$$

where: $f_c(\mathbf{x})$ is the objective function; $g_i(\mathbf{x})$ is the function of $i$-th constraint; $w_i$ is the weight coefficient of $i$-th constraint and $m$ is the number of constraints.

A logarithmic function has been applied as the constraints function [7]. The penalty correction has been introduced according to Powell-Skolnick method [14].

A program user-interface makes selection of the following parameters that are possible in the optimization procedure: the number of parents $\mu$; the offspring size $\lambda$; the number of generations $g$; and also the values of parameters of succumbed constraints and constraints weight coefficients. Moreover, selection of the crossover operator (uniform, proportional, biased) and mutation operator (utilization of random variables with Cauchy and Gauss distributions with appropriate choice of these distributions [7] and with chaotic distribution based on Lozi mapping [2]) is possible.

Figure 7 shows the program window for control of the optimization procedure. It is possible to determine parameter values as independent variables, their variation ranges, parameter values of succumbed constraints, as well as crossover and mutation operators.

As a result of the optimization procedure, the optimal solution vector and the full set of the optimal motor calculation results are offered. This set may be printed out or stored as a text file on the hard disc.

## 6. Conclusions

The presented computer software is a user-friendly and effective tool for the design of brushless DC motors with electronic commutation. Special effort has been made to facilitate the user to enter any changes to the magnetic circuit dimensions and winding parameters.

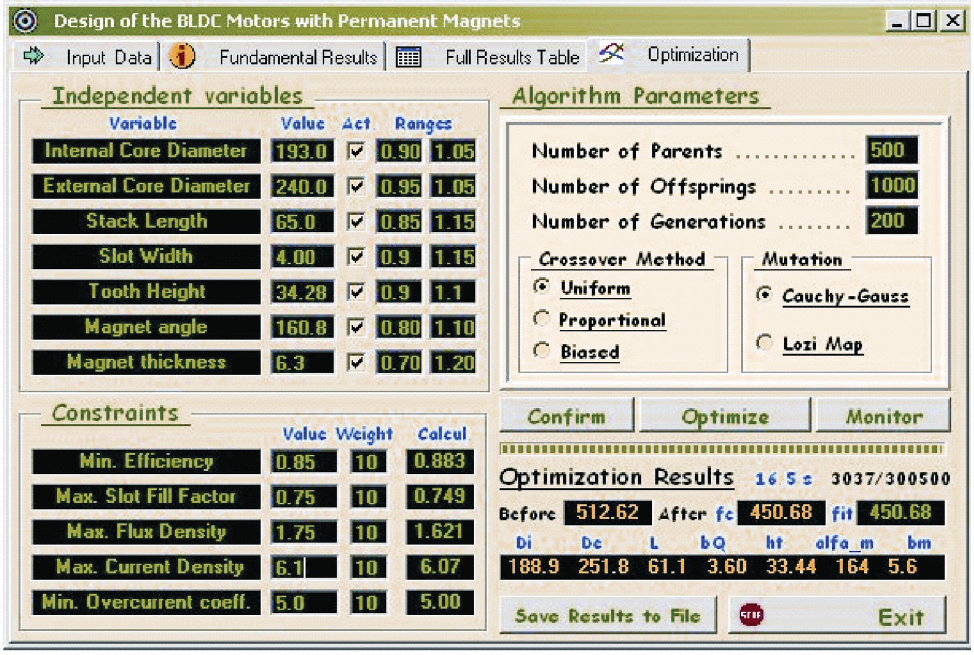

Independent variables

| Variable | Value | Act | Ranges | |
|---|---|---|---|---|
| Internal Core Diameter | 193.0 | ☑ | 0.90 | 1.05 |
| External Core Diameter | 240.0 | ☑ | 0.95 | 1.05 |
| Stack Length | 65.0 | ☑ | 0.85 | 1.15 |
| Slot Width | 4.00 | ☑ | 0.9 | 1.15 |
| Tooth Height | 34.28 | ☑ | 0.9 | 1.1 |
| Magnet angle | 160.8 | ☑ | 0.80 | 1.10 |
| Magnet thickness | 6.3 | ☑ | 0.70 | 1.20 |

Constraints

| | Value | Weight | Calcul |
|---|---|---|---|
| Min. Efficiency | 0.85 | 10 | 0.883 |
| Max. Slot Fill Factor | 0.75 | 10 | 0.749 |
| Max. Flux Density | 1.75 | 10 | 1.621 |
| Max. Current Density | 6.1 | 10 | 6.07 |
| Min. Overcurrent coeff. | 5.0 | 10 | 5.00 |

Algorithm Parameters

Number of Parents ............. 500
Number of Offsprings ......... 1000
Number of Generations ........ 200

Crossover Method
● Uniform
○ Proportional
○ Biased

Mutation
● Cauchy-Gauss
○ Lozi Map

Optimization Results 16.5 s 3037/300500

Before 512.62 After fc 450.68 fit 450.68

| Di | Dc | L | bQ | ht | alfa_m | bm |
|---|---|---|---|---|---|---|
| 188.9 | 251.8 | 61.1 | 3.60 | 33.44 | 164 | 5.6 |

Fig. 7. Program window for entering parameters, which control the optimization procedure

As a result, the program is designed and structured in such a way that interactive changes of parameters are possible via the user-interface. The user can simultaneously verify influences of these changes on the motor functional performance. Moreover, the software allows visualization of the back EMF per phase and shaft torque as functions of the rotor position angle.

Visual representation of these curves is helpful to estimate and select proper magnet angle $\beta$ and winding parameters, e.g., the number of slots per pole and the coil span. These parameters affect the torque ripple (cogging torque) and vibrations, which should be limited due to. imposed application requirements.

As an optimization method the non-deterministic evolution strategy procedure $(\mu + \lambda)$ – ES has been used. Owing to high prices of rare earth permanent magnets and negligible costs of consumption under operation, the minimal cost of active materials has been chosen as the optimization criterion.

## References

[1] J. Cichy, M. Dąbrowski, *Magnetic parameters evaluation of construction steels*. (in Polish) Archiwum Elektrotechniki XXIV(92): 329-343 (1975).

[2] L. Coelho, P. Alotto, *Electromagnetic device optimization by hybrid evolution strategy approaches. 9-th* Workshop on Optimization and Inverse Problems in Electromagnetism, Sorrento, 2006, COMPEL 26(2): 269-279 (2007).

[3] M. Dąbrowski, W. Szeląg, *Optimal sizing of permanent magnets*. (in Polish) Przegląd Elektrotechniczny: 396-399 (1981).

[4] M. Dąbrowski, *Analytical model of permanent magnets*. (in Polish) Zeszyty Naukowe Politechniki Poznańskiej. Elektryka 43: 5-23 (1994).

[5] M. Dąbrowski, *Analytical calculation methods of magnetic circuits with permanent magnets*. (in Polish) III Sympozjum *Zjawiska elektromagnetyczne w obwodach nieliniowych.* 58-67, Poznań 1975.

[6] M. Dąbrowski, *Permanent magnets interaction in electrical machines*. (in Polish) Międzynarodowa Konferencja *Maszyny elektryczne o magnesach trwałych.* 2: 5-22, Katowice 1979.

[7] M. Dąbrowski, A. Rudeński, *Application of the evolutionary algorithms for optimization of electrical machines.* Monografia ZKwE: 106-113 (2005).

[8] J.F. Gieras, *Permanent Magnet Motor Technology*. III Edition, CRC Press Taylor & Francis Group, New York 2009.

[9] J.F. Gieras, Rong-Je Wang, M.J. Kamper, *Axial Flux Permanent Magnet Brushless Machines*. Second Edition, Springer Science (2008).

[10] T. Glinka, *Electrical machines with permanent magnets*. (in Polish) Wyd. Politechniki Śląskiej, Gliwice 2002.

[11] D. Hanselman, *Brushless Permanent Magnet Motor Design*. Second Edition. The Writers Cillective, Cranston 2003.

[12] J.R. Hendershot, T.J.E. Miller *Design of Brushless Permanent Magnet Motors*. Clarendon Press, Oxford 1994.

[13] T. Li, G. Slemon, *Reduction of Cogging Torque in Permanent Magnet Motors*. IEEE Trans. on Magnetics 24(6): 2901-2903 (1988).

[14] D. Powell, M.M. Skolnick, *Using Genetic Algorithm in Engineering Design Optimization with Non-linear Constraints.* Proc. of the Fifth International Conference on Genetic Algorithms. ICGA'93: 424-430 (1993).

[15] A. Rudeński, *Problems of penalty function method in optimization of electrical machines by evolutionary methods*. (in Polish) Przegląd Elektrotechniczny 12: 73-78 (2007).